Molecular Crystals and Liquid Crystals Science and Technology. Section A. Molecular Crystals and Liquid Crystals

Publication details, including instructions for authors and subscription information:
http://www.tandfonline.com/loi/gmcl19

Electric Field Effects on Steady State and Time Resolved Fluorescence from Photosynthetic Reaction Centers

A. Ogrodnik [a]

[a] Institut für Physikalische und Theoretische Chemie, Technische Universität, München, D-8046, Garching

Version of record first published: 24 Sep 2006.

To cite this article: A. Ogrodnik (1993): Electric Field Effects on Steady State and Time Resolved Fluorescence from Photosynthetic Reaction Centers, Molecular Crystals and Liquid Crystals Science and Technology. Section A. Molecular Crystals and Liquid Crystals, 230:1, 35-56

To link to this article: http://dx.doi.org/10.1080/10587259308032211

Mol. Cryst. Liq. Cryst. 1993, Vol. 230, pp. 35–56
Reprints available directly from the publisher
Photocopying permitted by license only

Printed in the United States of America

ELECTRIC FIELD EFFECTS ON STEADY STATE AND TIME RESOLVED FLUORESCENCE FROM PHOTOSYNTHETIC REACTION CENTERS

A. OGRODNIK

Institut für Physikalische und Theoretische Chemie, Technische Universität München, D-8046 Garching

ABSTRACT A promising approach to identifying the primary electron acceptor and thereby the mechanism of primary charge separation in photosynthetic reaction centers (RCs) is the orientational determination of the dipole moment of the primary radical pair. This can be achieved by studying the angular dependence of the primary charge separation rate in an external electric field as reflected in the Dichroic Excitation spectrum of the eLectric Field modulated Yield of the prompt fluorescence (DELFY).

For RCs from *Rb.sphaeroides R-26* steady state, low temperature DELFY experiments point (within an angle of 5°) to the orientation of the dipole moment of $P^+H_A^-$. Time resolved fluorescence measurements revealed that the major contribution to the steady state fluorescence quantum yield and to the electric field effect thereon originates from a slow component with a lifetime of $\simeq$ 300 ps at 80K. This fluorescence component is by two orders of magnitude slower than the primary charge separation rate measured in absorption and might originate from a small ($\simeq$3%) subset of RCs characterized by slow, unistep charge separation.

Recent transient absorption measurements in electric fields revealed a significant reduction of the quantum yield of $P^+H_A^-$ formation within 30ps demanding a fast loss channel. In order to achieve dynamic competition with fast charge separation in the majority of RCs a more efficient loss channel than internal conversion is required, such as fast parking or trapping of excitation energy. From such a field modulated trapping state with the ability to fluoresce one would expect the observed loss of $P^+H_A^-$ quantum yield accompanied by a slow fluorescence component, which should be stronger than the measured one, however. This model would imply direct charge separation from $^1P^*$ to $P^+H_A^-$ in one step in the majority of RCs. Electric field induced charge separation to the B-branch forming $P^+B_B^-$ would better comply with the data, in case its energy is high enough to produce a quadratic field dependence of the delayed recombination fluorescence.

1. INTRODUCTION

Inspite of the remarkable progress in femtosecond spectroscopy of photosynthetic reaction centers (RCs), the mechanism of primary charge separation is not yet understood and the identity of the primary electron acceptor still under debate. In early femtosecond measurements[1-7] all spectral changes followed a single time constant consistent with a unistep[8-10], long range (17 Å) electron transfer (ET) from the excited bacteriochlorophyll dimer (P) to the bacteriopheophytin at the A-branch (H_A). The fast (2.8 ps at 300K) formation of $P^+H_A^-$ was subsequently explained by a superexchange mechanism involving the bacteriochlorophyll monomer (B) as mediator[11-22]. Consistency with nanosecond

recombination dynamics of $P^+H_A^-$ is only achieved when invoking conformational changes[21], however. More recent femtosecond measurements[23-26] reveal biphasic dynamics supporting a two-step primary ET. In this mechanism the primary rate determining ET proceeds from $^1P^*$ to B_A followed by the subsequent transfer[27-33] from B_A^- to H_A. These two models are extreme cases of more generalized treatments[34-40]. The basic difficulty in the experimental identification of an intermediate state $P^+B_A^-$ is the fact that the accumulation of the transient $P^+B_A^-$ remains small, since the second step was found to be at least a factor of four faster than the first one[1-7,23-26]. The discussion of the primary charge separation was further complicated by the observation of wavelength dependent femtosecond absorption data which were interpreted[40] in terms of an inhomogeneous distribution of primary ET rates. In RCs from *Chloroflexus aurantiacus* the situation is even more complex since a pronounced biphasic decay of the primary donor $^1P^*$ has been observed[41-43].

The wealth of high precision femtosecond spectroscopic data has not unambiguously elucidated the pathway of primary charge separation in RCs. This is less surprising, if one appreciates that the direct spectroscopic access to the potential intermediate $P^+B_A^-$ state may be obscured by a variety of phenomena and their mutual interplay, for example: (a) the superposition of main absorption bands, (b) nonspecific background absorption throughout the relevant spectral regions, (c) strong, overlapping and opposing electrochromic shifts in crucial spectral ranges, (d) significant excitonic coupling of the whole pigment system, (e) a small transient population of the possible intermediate $P^+B_A^-$, (f) processes such as intra- and inter-pigment nuclear relaxation and conformational changes of the protein dynamically affecting both spectral characteristics and ET dynamics (g) coherent optical effects in the ultra short time domain[44] and (h) a possible heterogeneity of RCs.

Most of these features are irrelevant when using methods which directly identify the orientation of the initially formed electric dipole moment and thereby the primary radical pair. This can be achieved via the response of the $^1P^*$ decay kinetics to an external electric field. By its very nature this approach is insensitive to the problems (a)-(g) and not affected by short lifetime or small transient concentration of a kinetic intermediate.

The method rests on the X-ray structural data available for RCs of *R. viridis*[8] and *Rb. sphaeroides*[9,10] and on the sensitivity of the ET rate on the free energy change which can be manipulated by the electric field: The free energy of the relevant radical pair changes with the scalar product $\mu.E$ of the interaction of the dipole moment μ with an externally applied electric field E. For this reason the free energy depends on the orientation of μ in the electric field, the directions of μ_B and μ_H differing by $\simeq 31^0$ in RCs of *R. viridis*[45]. As a consequence, the primary ET rate depends on the orientation as well. The orientation of the dipole moment of the initially formed radical pair can be determined from the angular dependence of the electric field effect on the primary charge separation rate with respect to the RC orientation in an external electric field. This idea was first reported by Lockhart et al.[46] together with an experimental attempt to measure the orientation of μ.

In RCs where the primary ET provides the dominant decay channel of the excited state $^1P^*$, any change of this rate is necessarily accompanied by a corresponding change of the quantum yield of the prompt fluorescence. Even in cases which do not allow the determination of this rate in absorption measurements, the rate can be monitored with the same precision as one can determine the prompt fluorescence yield. The first effort to obtain the angle between the primary dipole moment and the transition moment of fluorescence of $^1P^*$ consisted in measurements of the anisotropy of the fluorescence with respect to an external electric field under the condition of isotropic excitation[46]. This experimental approach suffered from two serious drawbacks: (a) Since the dipole moments of both radical pairs happen to project similarly onto the transition moment of fluorescence, no conclusions on the ET are possible from the angle under investigation[47]. (b) In addition to the relevant prompt fluorescence with ps lifetime, slow fluorescence components could contribute to or even dominate the steady state fluorescence signal. Such additional slow components may also be sensitive to electric fields.

In this paper the method of steady state **D**ichroic **E**xcitation spectrum of the e**L**ectric **F**ield modulated fluorescence **Y**ield (DELFY) is presented which can overcome the difficulty of discriminating between dipole moments accidentally projecting almost

identically onto the transition moment of fluorescence. By this method the angles κ (Figure 2b) of the effective dipole moment relative to various differently oriented transition moments are determined by spectral selection with the excitation light[45]. A DELFY spectrum is presented extending throughout the Q_x and Q_y transitions of both bacteriopheophytins and in the 880 nm special pair transition of RCs from *Rb.sphaeroides R-26* at 180K. In a second experiment, the possible contribution of slow components to the steady state fluorescence and the electric field effect thereon has been put to test in picosecond time resolved experiments. Various kinetic schemes compatible with these results and with recent transient absorption measurements in an electric field are discussed and the significance of DELFY measurements in each case is pointed out.

2. HOW DOES AN ELECTRIC FIELD INFLUENCE ELECTRON TRANSFER?

Depending on whether primary charge separation occurs in two steps or in one step enhanced by superexchange the radical pair first formed will be either $P^+B_A^-$ or $P^+H_A^-$, respectively. Due to the large distance of the radical ions, both radical pairs have large electric dipole moments amounting to $\mu_{P^+B_A^-}$ = 50 Debye and $\mu_{P^+H_A^-}$ = 82 Debye. These large dipole moments give rise to significant interaction with an externally applied electric field, as indicated in Figure 1. For example, a field of 1 10^6 V/cm will cause a maximal shift of the free energy of the radical pair states $P^+B_A^-$ and $P^+H_A^-$ by $\simeq$ 975 cm^{-1} and 1300 cm^{-1}, respectively, after correcting for the dielectric properties of the sample[62]. Strictly speaking, the free energy difference between the equilibrium configuration of the state prior to the ET process (with dipole moment μ_{P^*}) and after ($\mu_{D^+A^-}$) is

$$\Delta G = \Delta G_0 + (\mu_{P^*} - \mu_{D^+A^-}) \cdot E \tag{1}$$

with ΔG_0 being the free energy difference in absence of a field. μ_{P^*} can be estimated from the difference in dipole moments between ground and excited state $\Delta\mu$ as determined from Stark effect measurements ($\mu_{P^*} \simeq \Delta\mu$ = 8 Debye)[62,73,74].

As a consequence of changes in ΔG both the energy and the horizonal position of the transition state on the generalized reaction coordinate Q change. The change in free energy leads to a change of the activation energy $E_a(E)=(\Delta G(E)-\lambda)^2/4\lambda$ in the Franck-Condon factor of the ET rate:

$$k = V^2 \frac{1}{\sqrt{4\pi\lambda k_B T}} e^{\frac{-E_a(E)}{k_B T}} \tag{2}$$

The change in nuclear configuration of the transition state $Q_{ts}(E)$ may be reflected in a variation of the electronic coupling matrix element $V(Q_{ts}(E))$, if Born-Oppenheimer approximation is not strict. In case ET is enhanced due to superexchange coupling, additional variations are expected:

$$V(E)_{super} = \frac{V_{12}V_{23}}{\Delta E_V}(Q_{ts}(E)) \tag{3}$$

with V_{12} being the coupling between the initial state (P^*) and the mediator state ($P^+B_A^-$) and V_{23} being the coupling between the mediator state and the final state ($P^+H_A^-$). V_{super} depends on the electric field, since the vertical energy difference between the transition state and the multidimensional potential surface of the mediating state changes due to vertical shifts of the potential surfaces and due to horizonal motion of Q_{ts}. This complicated interplay is treated elsewhere in more detail[45].

According to (1) the interaction of the electric field with the vector of the effective electric dipole moment depends on their mutual orientation. This angular dependence is the basis for a method to determine the orientation of the primary formed radical pair, as described in the next chapter. This orientation can be compared with X-ray structural data in order to identify the pathway of primary charge separation.

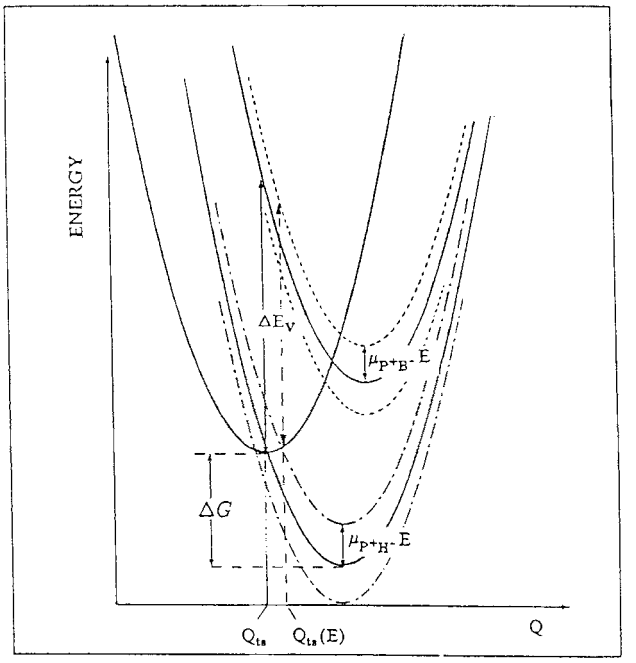

FIGURE 1: Simplified energy diagramm of an excited neutral state (P^*) prior to charge separation and of the radical pair state formed after ET ($P^+H_A^-$) together with a virtually populated radical pair intermediate ($P^+B_A^-$) as a function of reaction coordinate (Q) and their changes due to interaction of the radical pair states with an external electric field.

In a randomly oriented sample, the orientational dependence of the electric interaction gives rise to a continuous distribution of free energy differences, being reflected in a corresponding distribution of ET rates. The decay characteristics of the intrinsically heterogeneous sample have to be calculated by averaging over all possible orientations. The kinetics will be nonexponential, with decay components mostly being slower than without field and some being faster. In case the rate is activationless and can therefore not be further enhanced a dispersion only to slower timeconstants will be expected. Two different approaches have been made to handle the difficulties arising from such complex kinetics when studying the rather slow recombination of $P^+Q_A^-$. By fast modulation of the electric field during the ET process, effort has been made to isolate the electric field effect in an experimentally elegant way[64]. Alternatively, the kinetic trace has been analysed rigorously by numerical fitting making use of cumulant expansion[75,76]. Such analysis necessarily rests on an extreme reliability of experimental data with high dynamic range and very good linearity. Experiments in vectorially oriented RC preparations are very attractive[76], since they avoid this intrinsic heterogeneity.

3. THE DELFY METHOD

The orientational dependence of ET rates will be reflected in anisotropic properties of any signal related to such a reaction. In this context we consider the anisotropy monitored on changes of the fluorescence yield Φ of the primary donor $^1P^*$ assuming that these are mainly due to changes in the charge separation rate which is closely related to the lifetime of $^1P^*$.

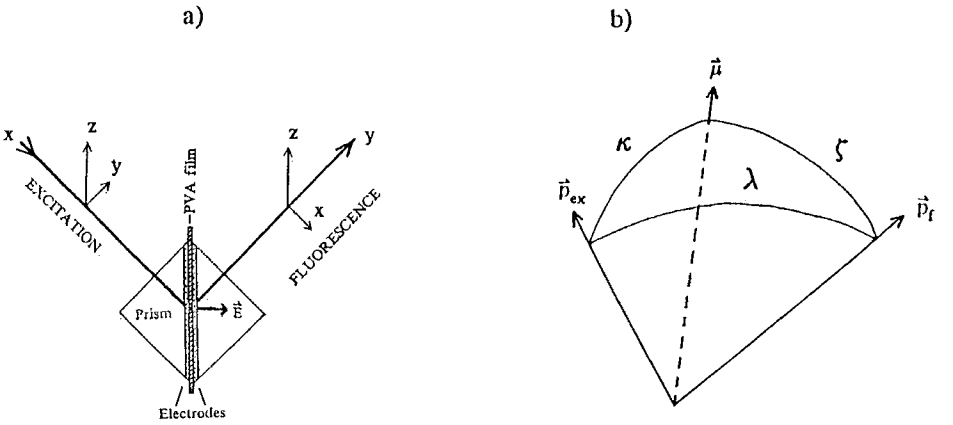

FIGURE 2: (a) Sample configuration: sample sandwiched between two prisms, providing refractive index matching for excitation beam (in x direction) and for emitting fluorescence (in y direction). Both excitation and emission enter the prism perpendicularly and the PVA film under 45°. Excitation may be polarized in the z and y direction and the fluorescence in the z and x direction. The electric field $\vec{E}$ is applied perpendicularly to the film by two electrodes. (b) Internal configuration of dipole moment μ, transition moment of excitation p_{ex}, and emission p_f spanning a tripod with the angles κ, ζ, and λ.

As will be shown later, prompt fluorescence makes only a minor contribution to the electric field effects, so that the results not necessarily refer to the primary charge separation process but could reflect the characteristics of a dipole moment involved in a competing loss process or in a recombination reaction. In this case this method can easily be extended to other more specific signals, like transient absorption changes. Unlike an earlier approach determining only a single projection angle of the orientation of the dipole moment influencing the monitor signal, the DELFY method is based on the selective excitation of appropriate transitions with polarized light, thereby achieving a defined orientational selection of RCs with respect to the electric field. In DELFY experiments all aspects of this anisotropy are registered completely leading to the full orientational information attainable.

Polarized excitation of selected transition moments photoselects RCs out of a given isotropic distribution. The assumption is made that energy transfer from any excited cofactor to P occurs exclusively within the same RC. Additional photoselection is achieved by detecting the fluorescence at a defined angle of polarization. These photoselection conditions define an orientational distribution of RCs with corresponding projections of the radical pair dipole moment onto the electric field direction and thus with corresponding changes of the fluorescence yield. Since different transitions with different projection angles κ can be selected by appropriate excitation wavelengths, the knowledge of the orientation of the transition moments enables the construction of the vector of the dipole moment of the primary radical pair in the coordinate system of the RC. According to the X-ray structural data[8-10], the various pigments in the RC supply transition moments which differ significantly in κ for the two possible states $P^+B_A^-$ and $P^+H_A^-$[47-49].

The magnitude of the electric field effect of the entirety of the RCs with respect to a given condition of photoselection has to be calculated by averaging over all possible orientations of the RCs. Such calculations are the theoretical basis of a DELFY experiment and have been worked out in detail[47]. In this averaging procedure a quadratic electric field dependence of the fluorescence change $\Delta\Phi = \Phi(E)-\Phi(0)$ was taken which has been shown to hold under our experimental conditions[46,48,49] up to fields of $\simeq 10^6$ V/cm. In isotropically

distributed RCs, linear contributions have to cancel due to mirror symmetry with respect to the electric field. Since the calculations have to be solved numerically, any other field dependence can easily be accounted for.

It has been recognized that the electric field on the fluorescence quantum yield, which per se are wavelength independent and rather large, are not simply superimposed on spectral shifts resulting from Stark effect, which per se leads to small effects. Their respective angular dependences can influence one another in a correlated way leading to complex field induced spectral features, which are considerably larger in amplitude than the Stark effect[50,51]. Such spectral shift, however, have not been observed in RCs[48-51], so that complications due to such effects are not expected. This is not surprising, since the effect occurs only under very special conditions.

In the context of this paper, the relevant quantity is the *anisotropy* of the electric field effect rather than its magnitude and field dependence. Therefore, uncertainties with respect to the local strength of the electric field do not affect the reliability of the method. However, the assumption has to be made that the distortion of the internal field due to the anisotropy of the dielectric properties is negligible.

The analysis of the electric field induced changes of the fluorescence yield under the condition of polarized excitation and emission has shown that the angle κ between the dipole moment of the primary radical pair and the transition moment of excitation can be deduced from the ratio[47] $\Delta\Phi(yx)/\Delta\Phi(zx)$. The electric field induced change of Φ given in the numerator refers to the geometry given in Figure 2 with the polarizations of excitation in y-direction and of fluorescence in the x-direction, the one in the denominator is with polarizations of excitation in z-direction and of fluorescence in x-direction. The difference in photoselection conditions can be appreciated by noting that for $\Delta\Phi(yx)$ the electric field vector is in the plane defined by the two directions of polarization, while for $\Delta\Phi(zx)$ it is

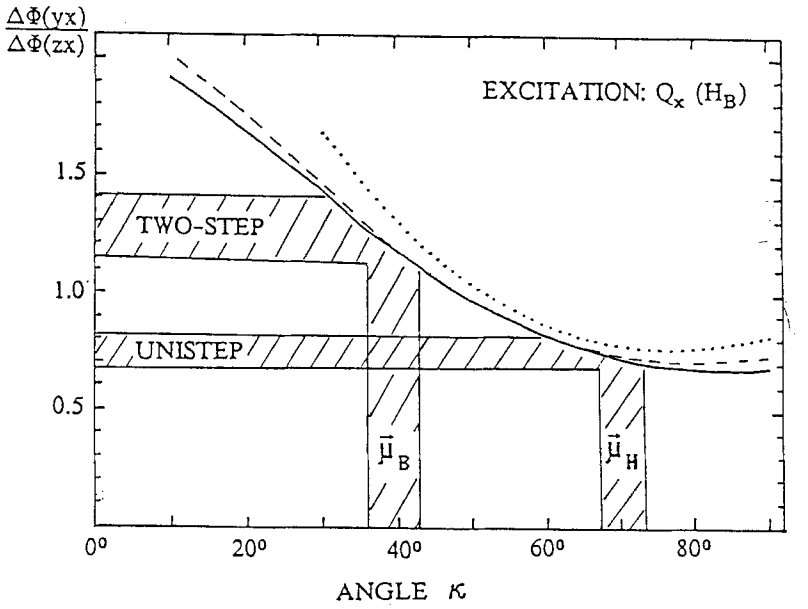

FIGURE 3: The electric field induced excitation anisotropy of the fluorescence yield $\Delta\Phi(yx)/\Delta\Phi(zx)$ as a function of κ with $\lambda=30^0$ (....), $\lambda=50^0$ (- - -) and $\lambda=70^0$ (----). ζ is fixed at $\simeq 60^0$ according to theoretical and experimental values for RCs of *Rb. sphaeroides* (see text). As an example, the angles κ between the transition moment of the Q_x band of H_B and the dipole moments μ_B and μ_H are marked.

out of the plane. Thus, the angle between polarization of absorption and the electric field changes from 45° to 90° while the angle between polarization of emission and the field remain unchanged at 45° in both cases. Thus the anisotropy ratio $\Delta\Phi(yx)/\Delta\Phi(zx)$ is most sensitive to the the orientation of the electric dipole moment μ with respect to the transition moment of excitation (angle κ), while in general it is only slightly sensitive to the angle (ζ) between μ and the transition moment of fluorescence. This weak sensitivity holds as long as the angle (λ) between the transition moment of excitation and emission is not too small, since then of course ζ and κ are identical and should reveal the same sensitivity. On rotating the polarization of excitation in the above defined way, the polarization vectors of excitation and emission remain orthogonal in both cases with the consequence that the detectability of the fluorecence in absence of an electric field remains unchanged as well, i.e. $\Phi(yx)/\Phi(zx)=1$ for E=0. This restriction dispenses us from normalizing both values of $\Delta\Phi$ and guarantees that $\Delta\Phi(yx)/\Delta\Phi(zx)$ is only weakly dependent on λ. This is illustrated by Figure 3, where the calculated dependence of $\Delta\Phi(yx)/\Delta\Phi(zx)$ on κ is shown for different values of λ, setting $\zeta\simeq 60°$. Due to the small slope of $\Delta\Phi(yx)/\Delta\Phi(zx)$ the discrimination of κ for large values of κ becomes more difficult. Analogously to the determination of κ, the value of ζ can be obtained from the ratio $\Delta\Phi(yx)/\Delta\Phi(yz)$ when the polarization of emission is rotated[45]. The value of $\zeta\simeq 60°$ measured at an excitation wavelength of 870 nm agrees with the one determined earlier[46].

In Table I the angles κ between the investigated transition moments and μ_{B_A} or μ_{H_A} are compiled together with the corresponding calculated values of $\Delta\Phi(yx)/\Delta\Phi(zx)$ from Figure 3. The bacteriochlorophyll transitions around 600nm and 800nm are omitted, because they overlap strongly and prohibit sufficient photoselection. The directions of the dipole

	μ_B (P^+B^-)		μ_H (P^+H^-)	
	angle κ	$\Delta\Phi(yx)/\Delta\Phi(zx)$	angle κ	$\Delta\Phi(yx)/\Delta\Phi(zx)$
Q_x (H_B)	39° ± 3°	1.25 ± 0.1	70° ± 3°	0.75 ± 0.07
Q_x (H_A)	20° ± 4°	$1.65^{+0.30}_{-0.15}$	49° ± 4°	$1.0^{+0.15}_{-0.10}$
Q_y (H_B)	48° ± 6°	1.05 ± 0.15	40° ± 6°	$1.2^{+0.25}_{-0.20}$
Q_y (H_A)	88° ± 3°	$0.70^{+0.20}$	58° ± 3°	$0.9^{+0.10}_{-0.12}$
Q_y (P)	57° ± 7°	$0.85^{+0.15}_{-0.10}$	61° ± 6°	0.82 ± 0.10

TABLE 1: The angles between the transition moments given in the first column an the dipole moments of either $P^+B_A^-$ or $P^+H_A^-$ together with the corresponding dichroic ratios $\Delta\Phi(yx)/\Delta\Phi(zx)$.

moments are based on electron density distributions according to quantum chemical calculations[47,52,53] and X-ray structural data[8-10]. In the Q_x region,the directions of transition moments were assumed to be parallel to the line connecting the nitrogen atoms in ring II and IV, being consistent with linear dichroic measurements[54]. In the Q_y region, we referred to the transition moments deduced from excitonic coupling[53]. Three of the transitions exhibit values of κ differing for μ_B and μ_H almost as much as the angle of 31° between μ_B and μ_H. As an example, the angles κ differing most for μ_B and μ_H, i.e. the one with respect to the Q_x transition of H_B at 530 nm, have been marked in Figure 3. For this transition the experimental value of $\Delta\Phi(yx)/\Delta\Phi(zx) = 0.85\pm 0.06$ has been determined earlier giving a value of $\kappa > 52°$ for RCs of *Rb. sphaeroides* R26 at low temperatures[48]. For the $Q_x(H_A)$ transition the angles κ are small and the small uncertainty in λ plays a larger role in this case. For the $Q_y(H_A)$ transition the values of κ are large. Due to the small slope of $\Delta\Phi(yx)/\Delta\Phi(zx)$ for large κ's in Figure 3 the discrimination becomes more difficult. Finally two points are emphasized:

(a) These dichroic ratios can in principle be time resolved.

(b) Analogous dichroic ratios can be defined for transient absorption signals. This holds in particular for the stimulated emission at 920 nm. However the time evolution of these ratios may be complicated.

4. EXPERIMENTAL FEATURES

STEADY STATE MEASUREMENTS

The excitation dichroism of the electric field modulated fluorescence yield was measured in a single photon counting fluorimeter in orthogonal geometry as described earlier[48]. The intensity of the exciting light was < 250 $\mu W/cm^2$, corresponding to $\simeq$ 0.2-1.0 turnovers/sec. Quinone containing RCs of *Rb.sphaeroides R-26* obtained by modified standard procedures were imbedded in PVA, yielding films of $\simeq$ 70 μm thickness with an optical density of 0.2 OD at 870 nm. The films were sandwiched between two rectangular prisms and two mylar foils, yielding a cube (Figure 2). The mylar foils were coated with optically transparent electrodes supplying the electric field, and were oriented together with the film in the diagonal of the cube. Two orthogonal faces of the cube were positioned perpendicularly to the directions of excitation and emission, thus eliminating refraction effects and orienting the electric field 45° to both directions. In order to avoid electrical breakdown, the temperature was kept below 180 K. Due to the low quantum yield of fluorescence from RCs ($4\ 10^{-4}$)[55], to losses in the monochromators and the polarization filters and to the low excitation intensity the counting rate of fluorescence was about 30 cts/sec. In order to achieve reliable signal to noise ratios in $\Delta\Phi(yx)/\Delta\Phi(zx)$, measuring times of more than 40 h were needed. Such long term measurements required automatic control and on line numeric normalization procedures. The measurement of the complete DELFY spectrum has been carried out in 30 cycles. The dichroic ratio defined above has the virtue of being insensitive to possible stray light and to field independent background fluorescence contributions, since they cancel, when differences $\Phi(E) - \Phi(0)$ are taken.

TIME RESOLVED MEASUREMENTS

For the time resolved measurements[82] the sample was excited at 864 nm with 40 ps pulses from a Hamamatsu PLP-01 laser diode at a repetition rate of 10 MHz. The excitation power was reduced with neutral density filters to 200 $\mu W/cm^2$ to avoid trapping of the RCs in the bottleneck state $P^+Q_A^-$. Sample geometry and electric field generation was the same as in the steady state experiment[48]. The light was gathered with an aspheric condensor lens and focused through two 920nm bandpass filters (bandwidth 20 nm) achieving an effective straylight rejection of $\simeq 10^{-7}$. Single photons were detected with a microchannel plate photomultiplier (Hamamatsu R2809U with S1-cathode) which was cooled to 190K in order to obtain a dark count rate of less than 2 cps. The fluorescence decay was measured using the time correlated single photon counting technique. The photomultiplier output was fed through an attenuator and an amplifier to a constant fraction discriminator supplying the

start pulse to a time-to-amplitude converter. This was read out by an 8K analog digital converter to a 32K multichannel analyzer. The stop pulse was obtained from the trigger output of the laser supply and controlling unit. The total instrument response function had a FWHM less than 50 ps. A measuring session of 8 h consisted of alternating 8 minute intervals in which either the response function was accumulated from the excitation light scattered off the sample or the 920 nm fluorescence response was accumulated. Initially the peak position of these response functions shifted considerably on the time axis. With a temperature stabilisation of the laser head and its power supply and control unit to ± 0.1° such drifts could be reduced to less than 11 ps. The residual shifts were taken into account before adding the fluorescence traces of the individual measuring intervals. Time traces in the presence and absence of the external electric field, which was modulated at 30 Hz, were accumulated simultaneously. For this purpose the multichannel analyser was modified in such a way that the incoming 8K data from the ADC were switched between two 8K segments by the electric field unit. Changes of the excitation pulse profile or residual drifts of the detection electronics are expected to affect both fluorescence decay traces in the same way. Taking the difference of the fluorescence signals with and without electric field should cancel such effects. This assumption was confirmed by the observation that the profiles of the instrumental response function with and without a field showed a maximum deviation of less than 10^{-3}.

5. STEADY STATE DELFY MEASUREMENTS

The relative electric field effect on the fluorescence is constant[48] throughout the fluorescence band of $^1P^*$. Contaminating fluorescence at 830 nm is well resolved, has low amplitude and completely lacks any electric field effect. The excitation spectra of the fluorescence detected at 905 nm and 930 nm were identical and reproduced the absorption spectrum of intact RCs, indicating that the fluorescence spectrum is homogeneous and that efficiency of energy transfer is rather constant for the various transitions of excitation. The isotropic electric field effect also is constant over the excitation spectrum between 520 nm and 880 nm. This means that if an electric field dependence of the efficiency of energy transfer from H and from B is present, it would have to be of similar magnitude. Energy transfer depends on the spectral overlap between donor and acceptor and its sensitivity to the Stark effect. Since the spectral overlap of B and H with P is completely different, the efficiency of energy transfer between these pigments should exhibit different sensitivity to the electric field. Because no dependence of the electric field effect on the excitation wavelength is found one can conclude that electric field induced changes of the energy transfer are small. Furthermore, it is known[65] that the quantum yield of energy transfer is near to unity. Thus, due to saturation in this regime the quantum yield would only weakly depend on changes of the energy transfer rates. In fact, the D_{LL} mutant lacking charge separation produced electric field effects 40-times smaller than in ordinary RCs for excitation of $^1P^*$ directly or via other pigments[56,57].

The excitation dichroism of the electric field effect on the fluorescence yield defined by the ratio $\Delta\Phi(yx)/\Delta\Phi(zx)$ was measured in the Q_x range of H_B (522-536 nm) and H_A (540-550 nm), the Q_y range of H_B (746-754 nm) and H_A (758-770 nm) and the special pair transition (866-882 nm). In Figure 4 the results obtained at 180K are shown. For comparison the expected ranges of $\Delta\Phi(yx)/\Delta\Phi(zx)$ corresponding to the dipole moments $P^+B_A^-$ and $P^+H_A^-$ given in Table 1 are marked. A good correlation of the experimental and theoretical values for the dipole moment $P^+H_A^-$ can be seen throughout the spectrum. In the two Q_x transitions the deviation from the theoretical values expected for $P^+B_A^-$ is significant. The Q_y transitions of the bacteriopheophytins are spectrally less clearly resolved than the Q_x transitions. Furthermore, in the Q_y region the theoretically expected values of $\Delta\Phi(yx)/\Delta\Phi(zx)$ partially overlap. Nevertheless, the experimental values tend to give better agreement with the data of $P^+H_A^-$. In the special pair transition the theoretical values for both dipole moments certainly do not allow a discrimination, but again are in good

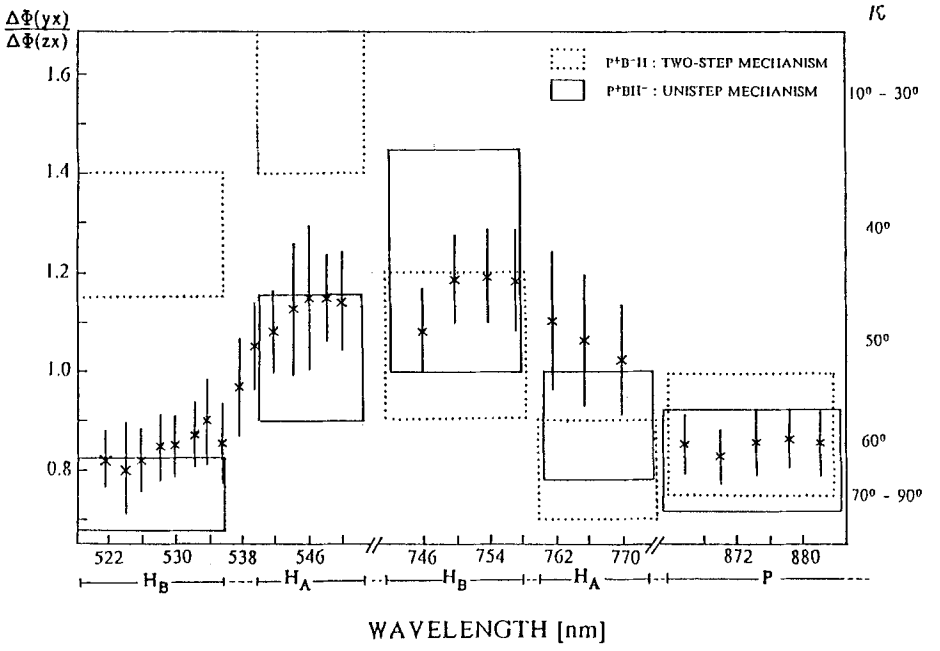

FIGURE 4: The dichroic excitation spectrum of the electric field modulated fluorescence yield in the Q_x and Q_y bands of the bacteriopheophytins and in the special pair band for RCs of *Rb. sphaeroides R-26* at 180 K. Left vertical scale: the dichroic ratio $\Delta\Phi(yx)/\Delta\Phi(zx)$, right vertical scale: corresponding angle κ (see Fig. 3). Ranges of values for the dichroic ratio according to Table 1 are marked by solid and dotted lines for $P^+H_A^-$ and $P^+B_A^-$ as the primary radical pair, respectively.

agreement with the experimental results. In the Q_x region, being particularly sensitive to the model of primary charge separation, measurements of $\Delta\Phi(yx)/\Delta\Phi(zx)$ have also been carried out at 80 K and essentially gave the same results[48].

From the data accumulated in Figure 4 five different projection angles κ onto the five inspected transition moments have been obtained from the theoretical dependence of $\Delta\Phi(yx)/\Delta\Phi(zx)$ on κ as indicated in Figure 3. The dependence of $\Delta\Phi(yx)/\Delta\Phi(zx)$ on κ was calculated numerically[45], setting $\zeta=60^0$. λ, the angle between the transition moment of excitation of the respective pigment and the transition moment of fluorescence of $^1P^*$, was calculated taking the transition moment of the 860nm absorption instead of the transition moment of emission. Our measurements of the dichroic ratio of the fluorescence on excitation at 860 nm showed the absorption and emission dipoles of $^1P^*$ to be parallel within 10^0 in agreement with earlier results[58]. Deviations of λ up to 20^0 can be tolerated without losing accuracy in determining the five angles κ. Two projection angles κ in general suffice to determine the orientation of the dipole moment of the primary radical pair. Therefore a unity vector representing that orientation was constructed by searching for the best match of all projection angles onto the transition moments with experimental values of κ in a least square fit. This fit resulted in an orientational vector for the dipole moment of the primary

radical pair with respect to the X-ray structure coordinate system[8] given below. For comparison the dipole vectors μ_B and μ_H are also shown.

$$\mu(\text{fit}) = \begin{pmatrix} 0.14 \\ 0.99 \\ 0.02 \end{pmatrix} \quad \mu_H = \begin{pmatrix} 0.225 \\ 0.974 \\ 0.035 \end{pmatrix} \quad \mu_B = \begin{pmatrix} 0.040 \\ 0.853 \\ 0.520 \end{pmatrix}$$

The deviation of the obtained vector μ(fit) from μ_H is 5.0° while it is 30.6° for μ_B. This result is convincing evidence that $P^+H_A^-$ is responsible for the observed electric field effect. The deviation of μ(fit) from μ_B is as large as the angle between μ_B and μ_H.

Since the orientation of μ can be established by two appropriate projection angles, our data set is overdetermining. The internal consistency of the data therefore demonstrates the justification of the assumptions made. In particular, this consistency becomes apparent in the Q_y region of H_B and P, where μ_B and μ_H are indistinguishable, because they have the same values of κ. The consistency confirms that:

(a) the orientations of the transition and dipole moments used in the calculations seem to be reasonable,

(b) the polarization is maintained within the RC,

(c) the orientation of the internal electric field at the pigment sites does not significantly deviate from the orientation of the externally applied field. Distinct orientational deviations at a certain atomic position have been calculated[59]. These might result from differences of the local fields at the individual atomic sites, and seem to average out over the total charge distribution of the dipole moment of the radical pair.

While results of DELFY measurements unambiguously demonstrate that the dipole moment $P^+H_A^-$ is responsible for the observed electric field effect, it is unclear how this influence on the steady state fluorescence is realized. There are two obvious problems associated with interpretation of the steady state fluorescence data:

a) They also contain possible contributions of delayed fluorescence from a recombination process $P^+H_A^- \rightarrow {}^1P^*H \rightarrow PH + h\nu$. These would give a trivial explanation for the findings given above since their electric field dependence would be dramatic.

b) Another fundamental problem of steady state measurements becomes evident, when we consider the possibility of a sample being heterogeneous with respect to the primary charge separation rate (Figure 6a). In such a case the various subpopulations contribute differently to the magnitude of the fluorescence signal: a decrease of the charge separation rate in a subpopulation leads to a proportional increase of the respective fluorescence quantum yield. Thus, we are faced with the possibility that a few RCs with slow charge separation kinetics dominate the fluorescence signal.

These possibilities will be discussed in more detail, after presenting time resolved fluorescence measurements in an electric field, which were performed to uncover the slow fluorescence components associated with such processes, and gaining further understanding about their contribution to the electric field effects.

6. TIME RESOLVED FLUORESCENCE MEASUREMENTS IN AN ELECTRIC FIELD

Time resolved fluorescence traces[82] measured at 80 K in presence F(t, E) and absence F(t, 0) of an electric field are shown in Figure 5a together with the time constants τ_i and relative quantum yields Φ_i obtained by a multi-exponential least square fit. Because of the large number of lifetimes needed to fit the data, a clear isolation of individual fluorescence components is not possible. Therefore the components referred to in the following should be treated as individuals only cautiously. Because of the logarithmic representation the distance between both traces, which have been accumulated simultaneously (see Methods), is proportional to the ratio F(t, E)/F(t, 0). The value is very small at short times and becomes maximal at about 2ns. The difference F(t, E)-F(t, 0), is shown in Figure 5b.

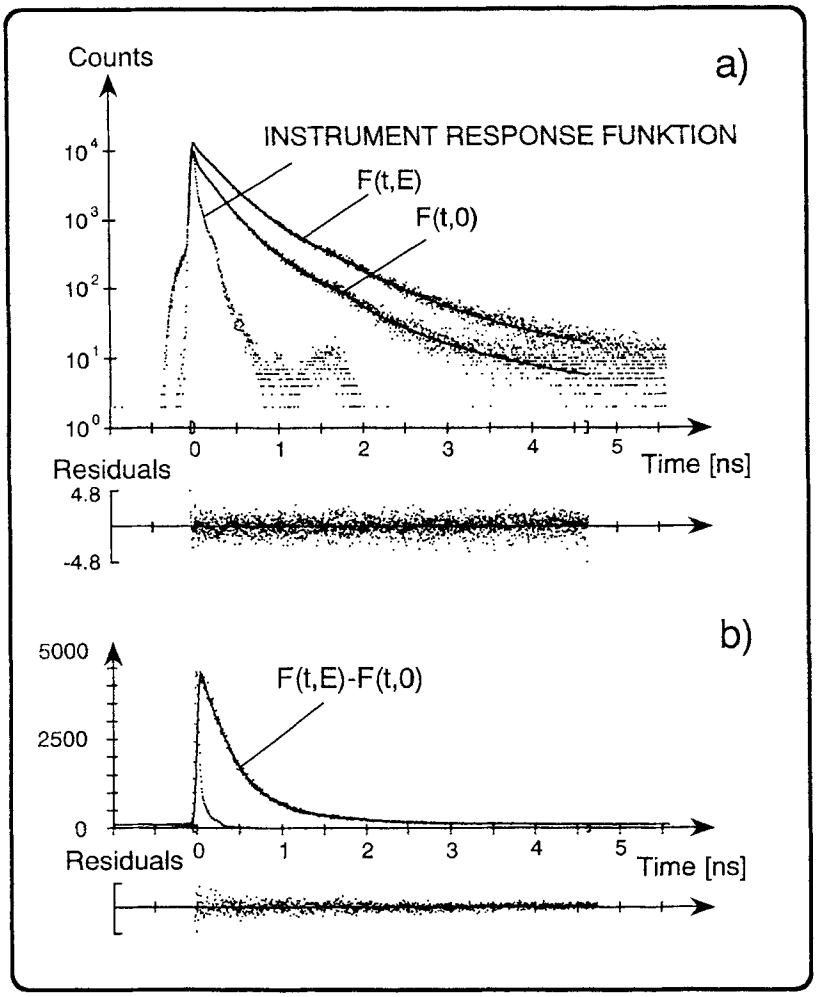

FIGURE 5: (a) Time resolved fluorescence traces F(t,0) in absence and F(t,E) in presence of an electric field of 1 10^6 V/cm detected at 920 nm after 865 nm excitation of RCs of *Rb. sphaeroides R-26* at 80 K. (b) Difference F(t,E)-F(t,0) of the fluorescence traces in presence and absence of electric field as given above. To avoid negative numbers not depictable in a logarithmic representation a constant value of 100 was added. Solid lines are multi-exponential fits of the data, with lifetimes τ_i and relative quantum yields Φ_i:

F(t,0):		**F(t,E):**		**F(t,E) - F(t,0):**	
τ_i	Φ_i	τ_i	Φ_i	τ_i	Φ_i
2	18.1%	2	18.6%	40	7%
130	26.6%	93	23.0%	331	58%
360	43.9%	300	86.8%	925	35%
850	8.9%	730	56.0%		
5200	2.4%	6400	6.5%		

In absence of a field the quantum yields are normalized to give $\Sigma\ \Phi_i = 1$. In presence of the field they are normalized by the same factor. In this case $\Sigma\ \Phi_i$ represents the modulation $\Phi_{tot(E)}/\ \Phi_{tot}(0)$ of the total steady state fluorescence which was 1.91.

Cursory inspection of the data immediately reveals that the main contribution to the fluorescence signal (≃44%) and a major contribution to the total electric field effect (43%) originates from a component having a lifetime of about 300 ps. An equally large contribution to the field effect of the overall quantum yield originates from a smaller component with 800 ps time constant being modulated in the field by a factor of 5, much more than any of the other components. The two fast components seem be field independent. This can clearly be deduced from the experimental data as long as only one single component is considered within the width of the response function of the apparatus. The contribution of the very fast fluorescence to the change of the total fluorescence can be judged more easily from its contribution to F(t,E)-F(t,0), since all emissions not sensitive to the electric field, e.g. scattered excitation light, cancel. There is no evidence at all for a very fast change in F(t,E)-F(t,0). A more adequate analysis of the electric field effects would have to account for the dispersion in lifetimes induced by the random orientation of the RCs in the electric field in a similar approach as demonstrated elsewhere[75,76]. Irrespective of this difficulty, two important statements can be summarized:

a) The fluorescence has considerable contributions from slow components. Its majority has a lifetime of about 300 ps.

b) The main contribution to the electric field effect originates from a 300ps and a 800ps component.

7. ADDITIONAL ELECTRIC FIELD EFFECTS

Very recently, additional experimental constraints for any model dealing with the primary kinetics and the electric field effects have been found in our group. The quantum yield of $P^+H_A^-$ formation ($\Phi_{P^+H_A^-}$) shows a pronounced decrease on application of an electric field[56,63]. Evidence for this fact has been deduced from transient absorption measurements of the bleaching at 546nm monitoring H_A and at 860nm monitoring P. An electric field induced reduction of the bacteriopheophytin bleaching appears within 30 ps, while a corresponding reduction of the dimer bleaching is not present at first, but evolves with a timeconstant of ≃ 900 ps. At fields of ≃ 7 10^5 V/cm a decrease of ≃11% occurred, while total fluorescence determined in the same samples with the same fields increased by ≃ 60%. This delayed recovery of the ground state absorption indicates that the loss channel does not lead to the ground state immediately. Instead, an intermediate state with a 900 nm lifetime has to be envisaged.

While these findings relate to quinone depleted RCs with further charge separation to the quinone blocked, measurements after 2 ns with quinone containing RCs exhibit a similar final loss in quantum yield of the $P^+Q_A^-$ state in agreement with Popovic et.al.[64]. In order to achieve a reduction in $\Phi_{P^+H_A^-}$ a loss channel has to be effectively competing with charge separation. The electric field would have to alter the branching ratio of $P^+H_A^-$ formation and the loss channel. Since the prompt fluorescence quantum yield, and consequently the average primary charge separation rate of the majority of RCs, does not change more than 50% the following problem arises: In order to achieve an average reduction of $\Phi_{P^+H_A^-}$ by 11%, the loss channel would have to be rather fast. A simple estimate yields an inverse loss rate[63] of ≃ 6-14ps. Obviously the maximum quantum yield in the absence of an electric field would be restricted to values of less than 85%, as long as significant field effects on the loss channel are not considered. This value barely complies with measurements[65] of $\Phi_{P^+Q_A^-}$. Internal conversion is not likely to be fast enough to account for such losses, since various measurements of the decay of the excited state of the bacteriochlorophyll dimer in systems lacking charge separation showed values of 200-600ps as the fastest time constant[56,66,81]. In the following the time resolved fluorescence data are discussed in view of the electric field effects detected in absorption.

8. DISCUSSION

WHAT IS THE NATURE OF THE SLOWER FLUORESCENCE COMPONENTS?

Prompt fluorescence is emitted from the radiating state immediately after its formation and directly reflects the excited state lifetime. In case part of the excitation energy can escape decay into the ground state and is stored in some long living state with no emission of its own, it will thermally repopulate the radiative state and lead to a slow emission termed *delayed fluorescence*. The lifetime and the amplitude of the delayed fluorescence reflects the lifetime and the energetic position of the storage state. In the following different possible sources for the slow fluorescence components will be discussed, which can be *prompt* in nature or *delayed*.

PROMPT FLUORESCENCE

The amplitude of the prompt fluorescence is determined by the radiative rate k_F. Its inverse lifetime is given by the sum of all decay rates. In this context discrimination is made between the field dependent charge separation with rate $k_1(E)$ being in general the main quenching rate and other loss rates $k_{loss}(E)$, which may be a) internal conversion the field dependence of which is small (<1.5% at 6 10^5 V/cm)[81] or b) ET routes alternative to normal charge separation, which may be strongly field dependent. As discussed in Chapter 2, the influence of the electric field depends on orientation. Therefore, the electric field $\vec{E}$ introduces an additional heterogeneity of $^1P^*$ lifetimes in an isotropic sample. Since the amplitude of the prompt fluorescence k_F is not sensitive[78] to E, the orientationally averaged lifetime:

$$\langle\tau(E)\rangle=\langle\frac{1}{k_1(E)+k_{loss}(E)}\rangle \tag{4}$$

determines the averaged yield of the prompt fluorescence:

$$\langle\Phi_{prompt}(E)\rangle=k_F\ \langle\tau(E)\rangle \tag{5}$$

In order to discuss prompt fluorescence components resulting from RCs with slow charge separation, we resort to inspect the obtained averaged quantum yield being proportional to the average change of lifetime, since we cannot reliably isolate individual fluorescence components with distinct time constants and therefore certainly cannot account for the additional heterogeneity in time constants introduced by the electric field.

NONFUNCTIONAL IMPURITIES: The simplest explanation for the slow fluorescence components is to attribute them to nonfunctional impurity pigments, i.e. to pigments not connected to RCs with intact charge separation. The fluorescence quantum yield of such pigments are influenced by: a) excitation probability proportional to the absorption cross section, b) k_F and by c) the internal conversion rate k_{IC}. However, no large dipole moments are involved in any of these processes. Both the absorption cross section and k_F are sensitive to the Stark effect, which is 4 orders of magnitude smaller than the effects measured on the fluorescence. The electric field sensitivity of internal conversion is smaller than a few percent. This has been demonstrated on excited bacteriochlorophyll dimers lacking charge separation, such as the D_{LL} mutant and B800/B850 antenna preparations[56,57,78,81]. Furthermore, the field effect in these systems turned out to have opposite sign to the ones in intact RCs. With the electric field effect of the time resolved fluorescence components being 100% and larger, a very useful fingerprint is at hand to decide, whether the source for the individual fluorescence component is connected to an ET process or not. Since the electric field changes observed here are substantial for all fluorescence components, the contribution from nonfunctional impurities is neglegible even for the nanosecond component.

HETEROGENEOUS CHARGE SEPARATION: As already discussed in Chapter 5, samples might contain a heterogeneous set of RCs with different rates of primary charge separation (Figure 6a). The time constants of some or all of the fluorescence components and their amplitudes would directly reflect the time constants of charge separation of the various components of the RC population and their relative proportions. From the small amplitudes of the slower fluorescence components, only a small minority of RCs with slower charge

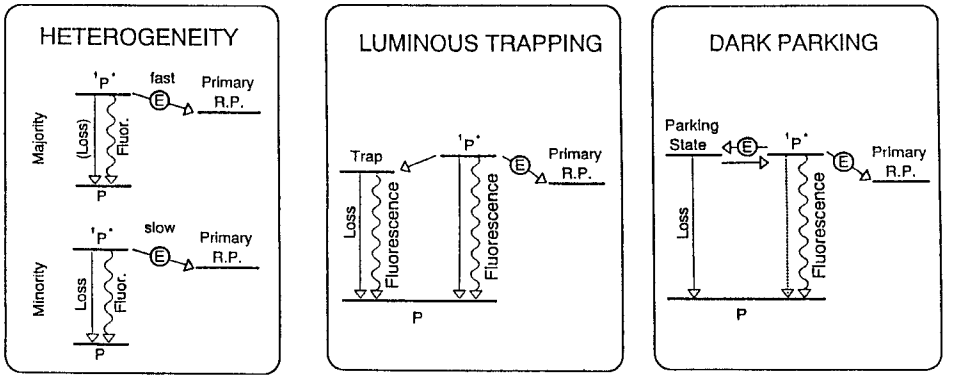

FIGURE 6: Three kinetic schemes illustrating the consequences of an electric field dependence of charge separation on fluoerecence quantum yield and loss of primary radical pair formation.
(a) HETEROGENEITY: Samples are heterogeneous consisting of RCs with fast or slow primary charge separation rates: a majority of fast RCs governs the signals obtained in transient absorption measurements. A minority of slow RCs is exposed to competing loss rates and is responsible for slow fluorescence components with high quantum yields.
(b) DARK PARKING: A parking mechanism (which may also be electric field sensitive) competes with primary charge separation. Delayed repopulation of $^1P^*$ produces delayed emisson components with amplitudes proportional to the equilibrium constant betwenn $^1P^*$ and parking state concentration. Losses in the parking state occur at the expense of primary radical pair formation.
(c) LUMINOUS TRAPPING: A trapping state with the ability to fluoresce will directly produce slow fluorescence components with considerably higher quantum yields than in (b), while primary radical pair loss is similarly effictive. The slow fluorescence components exhibit the same field dependence as the prompt fluorescence.

separation has to be envisaged. Such a minority of slowly charge separating RCs is compatible with the transient absorption data, since transient signals from this minority would be hidden by the transient changes due to the secondary ET from $P^+H_A^- \rightarrow P^+Q_A^-$. Thus, very sensitive transient absorption measurements in parallel with time resolved fluorescence measurements on quinone depleted samples would have to be conducted to prove this assumption. In case such a minority of slowly charge separating RCs were responsible for the observed electric field effect, the results of DELFY measurements then would be related to a minority of RCs in which charge separation occurs directly to $P^+H_A^-$ in one step. Such RCs would suffer considerable losses in quantum yield of charge separation $\Phi_{P^+H_A^-}$ on approaching the internal conversion lifetime being roughly[56,81] $1/k_{IC} \simeq$ 500ps, since then[63,79] $\Phi_{P^+H_A^-} = 1-\langle\tau(E)\rangle \cdot k_{IC}$. If the charge separation rate is small enough internal conversion will become the lifetime determining process. For any field independent loss channel (including internal conversion) the field effect on the fluorescence lifetime and consequently on its quantum yield will saturate. With decreasing k_1 the field induced increase in fluorescence quantum yield will become even smaller than the decrease

in quantum yield of $P^+H_A^-$ formation:

$$\frac{\langle\Phi(E)\rangle - \Phi(0)}{\Phi(0)} = - \frac{\langle\Phi_{P^+H_A^-}(E)\rangle - \Phi_{P^+H_A^-}(0)}{\Phi_{P^+H_A^-}(0)} \frac{k_1(0)}{k_{loss}} \quad (6)$$

This situation may be valid for the 300ps or for the 730ps component. Since prompt fluorescence of less than 2% of the RCs is able to account for the small amplitude of these components the corresponding losses in $\Phi_{P^+H_A^-}$ will not become evident in transient absorption measurements. Changes in $\Phi_{P^+H_A^-}$ were indeed only detected[63] at times earlier than 30ps. For the RCs being affected, the loss rate has to be faster[63] than ≃15ps. It is not clear whether the change in $\Phi_{P^+H_A^-}$ is a consequence of an average slowing down of $k_1(E)$ or a field induced increase of the effectiv k_{loss} of favourably oriented RCs. According to (4) such changes influence the $^1P^*$ lifetime and the prompt fluorescence in an antagonistic way. In order to neutralize both effects on the lifetime, the changes of $k_{loss}(E)$ would have to be larger than those of $k_1(E)$ as long as the later rate is dominant in (4) and no significant loss in $\Phi_{P^+H_A^-}$ (0) has to be considered. This could explain, why it was not possible to detect any major changes of the fluorescence in this time window. In such a picture, the electric field effects traced on the slow fluorescence would not be related to the decay of $^1P^*$ but to the decay of the intermediate state, as will be discussed below, or it would have a completely different origin. Consequently the obtained DELFY features would relate to a process different to charge separation.

LUMINOUS TRAPPING STATE: Instead of having a static heterogeneity of RCs with respect to their charge separation rates a dynamic conversion between fast and slow charge separation can prevail (Figure 6c). As an example, one may assume that the excited state $^1P^*$ exists in a form being *active* with respect to charge separation, and in a form being *inactive*, e.g. the $^1P^*$ state could be in a conformation adverse to charge separation. Assuming further that the radiative properties of such an *inactive* $^1P^*$ state do not change this state is called a luminous trapping state. Since such trapping states directly contribute to the fluorescence, their population is proportional to the *amplitude* of the associated fluorescence component. If one further assumes that after primary excitation essentially *active* $^1P^*$ states are formed, the electric field dependence of the slow fluorescence components can be understood. In the initially formed *active* states fast ET efficiently competes with loss to the trapping states, which fluoresce with high quantum yield while decaying slowly. Since the loss rate leading from *active* to the *inactive* state is not likely to be electric field dependent, only the field dependence of the charge separation rate together with its anisotropy are not only reflected in an increase of prompt fluorescence of the *active* state, but also in an average increase of the trapping population, an increase of the associated fluorescence component and an increase of the amount of ground state recovery with the same time constant.

A relatively weak temperature dependence of the slow fluorescence components[82] and their respective electric field effects imply that the trap for excitation energy is so deep compared to thermal energy that essentially no repopulation of the initial *active* state can occur. Alternatively, if the excitation energy can be transfered from an *active* state to *inactive* parking states having a certain probability of back transfer one must assume that a considerable amount of such *inactive* parking states exists, as compared to the amount of *active* $^1P^*$ states initially formed. Thus, the active states form a small region in phase-space, which is supposed to be initially occupied after excitation. If both *active* and *nonactive* states are isenthalpic, no pronounced temperature dependence of the balance between parking and *active* states will be expected. In phase space a certain part of the excitation energy diffuses away from the small *active* region, escaping charge separation and getting lost in the expanse of *inactive* states before it decays via slower non-radiative channels, such as internal conversion. Since the essential feature of this model is the excitation energy getting trapped due to the entropy effect, these states are called traps, as well. A third explanation for the missing temperature dependence could result from saturation effects as will be discussed in

connection with delayed fluorescence.

In the first two cases the amplitude of the slow fluorescence is determined by the initial branching ratio of the *active* route to the *inactive* one. This has the important consequence, that the slow fluorescence component essentially shows the same electric field dependence as expected for the early 2ps fluorescence, and of course the same DELFY features. The relatively large electric field effects on the quantum yield of $P^+H_A^-$ can readily be explained in case the trapping rate competes efficiently with charge separation. The special pair ground state absorption (860nm) initially remains fully bleached in the electric field since it merely converts to its *nonactive* excited state. Together with the decay of these trapping states the ground state recovers to a proportional degree and therefore exhibits the electric field effect with a corresponding delay. The 11% effect on $P^+H_A^-$ calls for a correspondingly large amplitude of the delayed fluorescence which has to be at least 11% of that of the prompt fluorescence (as long as k_F is assumed to be the same in the *active* and *inactive* state). Experimentally the 300ps component is by a factor of 3, the 730ps component by a factor of 12 smaller than this minimum value, however. Thus, as long as our determination of prompt fluorescence is not overestimated by unresolved fast fluorescence contributions different from prompt fluorescence, at least the 730ps component does not relate to a luminous trapping state. Another crucial objection to this state is the missing of any observable field effect on the prompt fluorescence, which should parallel that of the slow component from the *inactive* state, as pointed out above. According to the 300ps or the 730ps components a 2-fold or a 6-fold increase of the prompt fluorescence would be expected. Even if additional fluorescence components are hidden under the 2 ps component fitted to the data, it is quite out of question, that they could mask the expected 6-fold change, at least.

DELAYED FLUORESCENCE

Slow fluorescence components in general arouse suspicion of being delayed fluorescence. It will be shown that delayed fluorescence is particularly sensitive to electric field effects. The origin of these fluorescence components may either be radical pair states which may be formed after normal charge separation: $P^+B_A^-$, $P^+H_A^-$ or $P^+Q_A^-$. Alternatively, dark parking states (Figure 6b) may be formed in competition with normal charge separation, as indicated by the transient absorption data referred to above. In contrast to the luminous trapping state, these states have no fluorescence of their own (dark) but they can repopulate (parking) $^1P^*$ producing fluorescence components following their lifetime.

For both cases the quantum yield of such a delayed fluorescence can roughly be estimated by following a derivation presented elsewhere[60]:

$$\Phi_{delayed} = k_F \exp(-(\Delta G+\mu \cdot E)/kT)\, p^2(E)\, \tau_{delayed}(E) \qquad (7)$$

The delayed fluorescence amplitude is proportional to the radiative rate k_F, to the probability p(E) of the delayed state being formed in competition to normal charge separation, and to the Boltzmann factor expressing the probability of thermal repopulation of $^1P^*$. ΔG is the free energy separation between the delayed state and $^1P^*$. The second factor of p(E) refers to the parking state only and accounts for the fact that it is not in equilibrium with $^1P^*$ ($k_{loss} < k_1$) and that therefore the parking state is repopulated only with the probability p(E) after thermal reformation of $^1P^*$.

As discussed earlier, k_F can be treated as field independent. For a radical pair on the A-branch (e.g. $P^+H_A^-$) p is close to unity because of the high quantum yield of charge separation. According to the transient absorption data p(E) is expected to reduce by about 11% in high fields. In case the delayed state is a parking state off the normal charge separation route and is formed with the rate k_{loss}, then $p(E) = k_{loss}(E)/(k_1(E)+k_{loss}(E)+k_{ic})$. This p value for the parking state is just 1 minus the p value for the $P^+H_A^-$ state. Accounting for the direct decay rate of the delayed state to the ground state k_g, which is assumed to be field independent, and for activated decay via $^1P^*$, the delayed lifetime, which is experimentally accessible, is determined by:

$$\tau_{delayed}(E) \simeq \frac{1}{k_g + (1-p(E))\exp\left(-\frac{\Delta G+\mu\cdot E}{kT}\right)k_{loss}} \quad (8)$$

The contribution of delayed fluorescence as compared to prompt fluorescence can be significant if the lifetime of delayed state is large enough to compensate the reduction of its amplitude due to the Boltzmann factor. The influence of the electric field on the energy level of the delayed state can lead to dramatic changes in the Boltzmann factor, since at an external field of 6 10^5 V/cm a value of $\mu\cdot E \simeq 960\ cm^{-1}$ (120 meV) is obtained, which is much larger than kT at all temperatures. The contribution of the Boltzmann factor has to be averaged over all orientations of μ with respect to the electric field yielding a superquadratic field dependence for $\Phi(E)/\Phi(0)_{delayed} = \langle\exp(-\mu\cdot E/kT)\rangle = (kT/\mu\cdot E)\sinh(\mu\cdot E/kT)$, as long as $\Delta G+\mu\cdot E < kT$. Note that the relative change of this fluorescence component is independent of the energy gap between the fluorescing and the radical pair parking state. ΔG determines the absolute value of the delayed amplitude and of its absolute change. For $\mu\cdot E > kT$ an expansion of the field dependence cannot be terminated at the quadratic term but considerable deviations from a quadratic field dependence would be expected. Furthermore, the electric field induced change of a delayed fluorescence contribution should reveal a strong temperature dependence. However, as soon as the Boltzmann factor gets close to 1, not only the amplitude increases but also $\tau_{delayed}$ decreases. For the quantum yield both actions cancel. Therefore, the E-dependence is expected to saturate at sufficiently high fields. Within the noninverted region k_{loss} will decrease rapidly when the parking state is shifted to higher energies and so will p(E).

Since none of the fluorescence components exhibits a superquadratic field dependence and the field effects show no temperature dependence[50,80] the conclusion is madethat either the observed fluorescence components are not associated with a radical pair or parking state or that the free energy gap to $^1P^*$ is not larger than $\mu\cdot E$. A more rigorous treatment of the interplay of $\mu\cdot E$, ΔG and kT on influencing the delayed fluorescence trace for an average of all orientations is in preparation.

$P^+H_A^-$: Earlier, various delayed fluorescence components have been ascribed[67] as recombination fluorescence of nonrelaxed radical pair states $P^+H_A^-$. Since in the RCs investigated here the reaction $P^+H_A^- \rightarrow P^+Q_A^-$ was not blocked the lifetime of the $P^+H_A^-$ state is shorter than the time during which the main contribution to the fluorescence and its electric field effect prevails. Time resolved measurements of the fluorescence decay with less time resolution revealed slow fluorescence components only in blocked RCs, while the fluorescence trace of unblocked RCs was taken for the response function of the apparatus[67]. The present data confirms the view taken earlier[60], that it is not advisable to make use of a response function derived in such a way, since both preparations have similar components in the ps- and ns-time range. A more quantitative evaluation has to compare the amplitude of these components with the prompt fluorescence, or the yield of these components in blocked and unblocked RCs[60,67] and is in progress.

DARK PARKING STATE: The fact, that the electric field effect on the fluorescence does not depend strongly on whether ET to the quinone is blocked or not is compatible with the notion that part of the excitation energy is stored in parking states. As shown in the Caption to Figure 5 the ratio of the amplitudes of the delayed fluorescence to that of the prompt one are ≃0.03 for the 300ps component and ≃0.008 for the 730ps component. This ratio is given by Eq. (7) to be $\exp(-(\Delta G+\mu\cdot E)/kT)\ p^2(E)$. Transient absorption measurements limit the average probability $\langle p(E)\rangle$ of forming a parking state to values smaller than ≃11%. Thus, the Boltzmann factor would have to be very close to 1 for the parking state. In this case the electric field dependence is expected to be dominated by p(E). Depending on the interplay of $k_1(E)$ and $k_{loss}(E)$ the orientation of the effective dipole moment determined in DELFY measurements will have the characteristics of the primary radical pair or of the parking state or some combination of both. An obvious candidate for a dark parking channel would be

charge separation to the B-branch. However, no evidence for electric field induced $P^+H_B^-$ formation could be deduced from transient absorption measurements[56,63,70] in the Q_x band, where both pheophytins can be discriminated. Very recent measurements around 800nm, however, indicate that a bacteriochlorophyll monomer is involved in the parking state, suggesting it is $P^+B_B^-$[79]. If the slow fluorescence components indeed relate to $P^+B_B^-$ one would conclude from the orientation of the effective dipole moment determined in the DELFY experiment that the dipole moment of $P^+B_B^-$ does not play a significant role for the electric field effect on the delayed fluorescence, since it deviates by more than 110° from the measured one. In this case p(E) would be dominated by the field effect of $k_1(E)$ and not of $k_{loss}(E)$ forming $P^+B_B^-$. On the other hand, if the field effect on k_{loss} dominates, one could even comply with high quantum yields in absence of a field. The dipole moments associated with A- and B-branch charge separation will act on the competing reactions $k_1(E)$ and on k_{loss} in an antagonistic way. For properly oriented RCs the field will slow down ET to the A-branch and enhance ET to the B-branch. For this fraction the expected increase of the quantum yield of prompt fluorescence due to slowing down at the A-branch may partially be compensated by speeding up at the B-branch. At the same time the quantum yield of the loss channel is enhanced by both effects. For a better understanding a careful analysis of the complete orientational dependence of individual fluorescence components and a comparison with DELFY detected in transient absorption is yet necessary.

9. CONCLUSIONS

The measured steady state DELFY spectrum exposes an electric dipole moment which is parallel in space to that of $P^+H_A^-$. The time resolved fluorescence data show that the detected field effects refer to fluorescence components much slower than the primary charge separation rate and are therefore at least not directly related to it. In spite of a whole series of experiments in electric fields, no conclusion on the ET mechanism can yet be made for the bulk of the RCs.

Within the scope of this work one cannot exclude the possibility that the detected electric field effects originate from a minority of RCs accomplishing only slow charge separation directly to $P^+H_A^-$, as reflected by the slow fluorescence components. In this case another, more efficient mechanism would have to account for the field effects on $P^+H_A^-$ formation. Alternatively, it is suggested that a larger fraction of RCs with a broadly dispersed distribution of slow charge separation rates could comply with both fluorescence and transient absorption measurements. More likely, the magnitude of the field effect on $P^+H_A^-$ reflects losses in the bulk of RCs. The fast charge separation rate in these RCs demands a correspondingly fast loss channel. Since internal conversion is presumably too slow, fast parking or trapping of excitation energy has to be envisaged. For the slow fluorescence components a luminous trapping state tends to yield amplitudes being too large, while a dark parking state yields rather low amplitudes, unless this state is energetically very close to $^1P^*$. In this case the unexpectedly weak electric field dependence of the fluorescence components would result from saturation effects. The radical pair $P^+B_B^-$ seems to be an interesting candidate for such a parking state.

There is no doubt, that the possibility of directly influencing primary charge separation with an electric field gives us an attractive access to the mechanism of primary charge separation. The reason why this question remains open is the limited time resolution of the present experiments. These measurements did, however, indicate that the presently discussed kinetic scheme of the very fast processes in the RCs, as deduced from fs-transient absorption experiments alone, is incomplete.

Transient absorption and emission measurements with the appropriate time resolution and sensitivity should be able to trace the influence of the electric field on charge separation directly. As demonstrated in this paper, the electric field effect is an excellent fingerprint for unravelling superimposed signals. Thus, it should be useful in deciding the unsettled issues in the kinetic interpretation of transient signals referred to in the introduction. In particular, a time resolved DELFY experiment or a corresponding dichroic absorption

experiment in an electric field should be able to establish the mechanism of primary charge separation and further reveal loss channels overlooked so far. One should try to trace formation and decay of the proposed parking or trapping states in absence of a field and analyse the the field dependence of these kinetics. Investigations on mutants with slow charge separation should reveal such parking or trapping states more clearly, since then larger losses in quantum yield of $P^+H_A^-$ in presence and absence of an electric field are expected.

ACKNOWLEDGEMENT

I want to thank Prof. M.E. Michel-Beyerle, Dr. U. Eberl, Dr. M. Volk and all my other colleques involved in the work which was compiled in this paper. Financial support from the Deutsche Forschungsgemeinschaft (Sonderforschungsbereich 143) is gratefully acknowledged.

REFERENCES

1. J.-L. Martin, J. Breton, A.J. Hoff, A. Migus and A. Antonetti, Proc. Natl. Acad. Sci. USA, 83, 957 (1986).
2. J. Breton, J.-L. Martin, G.R. Fleming and J.-C. Lambry, Biochemistry, 27, 8276 (1988).
3. G.R. Fleming, J.-L. Martin and J. Breton, Nature, 333, 190 (1988).
4. J. Breton, J.-L. Martin, J. Petrich, A. Migus and A. Antonetti, FEBS Lett., 209, 37 (1986).
5. J.-L. Martin, J. Breton, A.J. Hoff, A. Migus and A. Antonetti, Proc. Nat. Acad. Sci. USA, 83, 957 (1986).
6. N.W. Woodbury, M. Becker, D. Middendorf and W.W. Parson, Biochemistry, 24, 7516 (1985).
7. C. Kirmaier, D. Holten and W.W. Parson, FEBS Lett., 185, 76 (1985).
8. J. Deisenhofer, H. Michel, EMBO J., 8, 2149 (1989).
9. H. Komiya, T.O. Yeates, D.C. Rees, J.P. Allen and G. Feher, Proc. Natl. Acad. Sci. USA, 85, 9012 (1988).
10. D.E. Budil, P. Gast, C.-H. Chang, M. Schiffer and J.R. Norris, Ann. Rev. Phys. Chem., 38, 561 (1987).
11. S.F. Fischer, I. Nussbaum and P.O.J. Scherer, in Antennas and Reaction Centers of Photosynthetic Bacteria, edited by M.E. Michel-Beyerle (Springer, Berlin, 1985), pp. 256-263.
12. J. Jortner and M.E. Michel-Beyerle, in Antennas and Reaction Centers of Photosynthetic Bacteria, edited by M.E. Michel-Beyerle (Springer, Berlin, 1985), pp. 345-365.
13. J. Jortner and M. Bixon, in Protein Structure Molecular and Electronic Reactivity, edited by R. Austin, E. Buhks, B. Chance, D. DeVault, P.L. Dutton, H. Frauenfelder and V.I. Gol'danskii (Springer, New York, 1987), pp. 277-308.
14. A. Ogrodnik, N. Remy-Richter, M.E. Michel-Beyerle and R. Feick, Chem. Phys. Lett., 135, 576 (1987).
15. J.R. Norris, D.E. Budil, D.M. Tiede, J. Tang, S.V. Kolaczkowski, C.H. Chang and M. Schiffer, in Progress in Photosynthetic Research I, edited by J. Biggens (Martinus Nijhoff, Dordrecht, 1987), pp. 363-369.
16. M.E. Michel-Beyerle, M. Plato, J. Deisenhofer, H. Michel, M. Bixon and J. Jortner, Biochim. Biophys. Acta, 932, 52 (1988).
17. M. Bixon, J. Jortner, M. Plato and M.E. Michel-Beyerle, in The Photosynthetic Bacterial Reaction Center. Structure and Dynamics, edited by J. Breton and A. Vermeglio (Plenum, New York., 1988), pp. 399-420.
18. M. Plato, K. Möbius, M.E. Michel-Beyerle, M. Bixon and J. Jortner, J. Am. Chem. Soc., 110, 7279 (1988).
19. M.E. Michel-Beyerle, M. Bixon and J. Jortner, Chem. Phys. Lett., 151, 188 (1988).
20. M. Bixon, M.E. Michel-Beyerle and J. Jortner, Isr. J. Chem., 28, 155 (1988).

21. M. Bixon, J. Jortner, M.E. Michel-Beyerle and A. Ogrodnik, Biochim. Biophys. Acta, 977, 273 (1989).
22. R.A. Friesner and Y. Won, Biochim. Biophys. Acta, 977, 99 (1989).
23. W. Holzapfel, U. Finkele, W. Kaiser, D. Oesterhelt, H. Scheer, H.U. Stilz and W. Zinth, Chem. Phys. Lett., 160, 1 (1989).
24. W. Holzapfel, U. Finkele, W. Kaiser, D. Oesterhelt, H. Scheer, H.U. Stilz and W. Zinth, Proc. Natl. Acad. Sci. USA, 87, 5168 (1990).
25. C. Lauterwasser, U. Finkele, H. Scheer and W. Zinth, Chem. Phys. Lett. 183, 471 (1991).
26. C.-K. Chan, T.J. DiMagno, L.X.-Q. Chen, J.R. Norris and G.R. Fleming, Proc. Nat. Acad. Sci. USA, 88, 11202 (1991).
27. R.A. Marcus, Isr. J. Chem., 28, 205 (1988).
28. R. Haberkorn, M.E. Michel-Beyerle and R.A. Marcus, Proc. Natl. Acad. Sci. USA, 70, 4185 (1979).
29. R.A. Marcus, Chem. Phys. Lett., 133, 471 (1987).
30. S.V. Chekalin, Ya.A. Matveetz, A.Ya. Shkuropatov, V.A. Shuvalov and A.P. Yartzev, FEBS Lett., 216, 245 (1987).
31. S.F. Fischer and P.O.J. Scherer, Chem. Phys., 115, 151 (1987).
32. R.A. Marcus, Chem. Phys. Lett., 146, 13 (1988).
33. S. Creighton, J.-K. Hwang, A. Warshel, W.W. Parson and J. Norris, Biochemistry, 27, 774 (1988).
34. M. Bixon, J. Jortner and M.E. Michel-Beyerle, Biochim. Biophys. Acta, 1056, 301 (1991).
35. R. Marcus and R. Almeida, J. Phys. Chem., 94, 2973 (1990).
36. R. Almeida and R. Marcus, J. Phys. Chem., 94, 2978 (1990).
37. Yu. Hu and S. Mukamel, J. Chem. Phys., 91, 6973 (1989).
38. M. Sugawara, Y. Fujinura, O. Yeh and S.H. Lin, J. Photochem. Photobiol., 54, 321 (1990).
39. Y.I. Kharkhats and J. Ulstrup, Chem. Phys. Lett., 182, 81 (1991).
40. Ch. Kirmaier and D. Holten, Proc. Natl. Acad. Sci. USA, 87, 3552 (1990).
41. J.-L. Martin, J.C. Lambry, M. Ashokkumar, M.E. Michel-Beyerle, R. Feick and J. Breton, in Ultrafast Phenomena VII, edited by Harris, Ippen (Springer, Berlin, 1990).
42. R. Feick, J.-L. Martin, J. Breton, M. Volk, G. Scheidel, T. Langenbacher, C. Urbano, A. Ogrodnik and M.E. Michel-Beyerle, in Reaction Centers of Photosynthetic Bacteria, edited by M.E. Michel-Beyerle (Springer, Berlin, 1990), pp. 181-188.
43. M. Becker, V. Nagarajan, D. Middendorf, W.W. Parson, J.E. Martin and R.E. Blankenship, Biochim. Biophys. Acta, 1057, 299 (1991).
44. M.H. Vos, J.-C. Lambry, S.J. Robles, D.C. Youvan, J. Breton and J.-L Martin, Proc. Natl. Acad. Sci. USA, 88, 8885 (1991).
45. D.J. Lockhart, R.F. Goldstein and S.G. Boxer, J. Chem. Phys., 89, 1408 (1988).
46. A. Ogrodnik and M.E. Michel-Beyerle, Z. Naturforsch., 44a, 763 (1989).
47. U. Eberl, A. Ogrodnik and M.E. Michel-Beyerle, Z. Naturforsch., 45a, 763 (1990).
48. A. Ogrodnik, U. Eberl, R. Heckmann, M. Kappl, R. Feick, M.E. Michel-Beyerle, J. Phys. Chem., 95, 2036 (1990).
49. A. Ogrodnik, U. Eberl, R. Heckmann, M. Kappl, R. Feick and M.E. Michel-Beyerle, in Reaction Centers of Photosynthetic Bacteria, edited by Michel-Beyerle (Springer, Berlin, 1990), pp. 157-168.
50. D.J. Lockhart, Ch. Kirmaier, D. Holten and S.G. Boxer, J. Phys. Chem., 94, 6987 (1990).
51. S.G. Boxer, D.J. Lockhart, S. Franzen and S.H. Hammes, in Reaction Centers of Photosynthetic Bacteria, edited by M.E. Michel-Beyerle (Springer, Berlin, 1990), pp. 147-156.
52. M. Plato, W. Lubitz, F. Lendzian and K. Möbius, Isr. J. Chem., 28, 109 (1988).
53. P.O.J. Scherer and S.F. Fischer , in Perspectives in Photosynthesis, edited by J. Jortner and B. Pullman (Kluwer, Dordrecht 1990), pp. 361-370.
54. J. Breton, in The Photosynthetic Bacterial Reaction Center - Structure and Dynamics,

edited by J. Breton and A. Vermeglio (Plenum Press, New York and London, 1988), pp. 59-60.
55. K.L. Zankel, D.W. Reed and R.K. Clayton, Proc. Natl. Acad. Sci. USA, 61, 1243 (1968).
56. A. Ogrodnik, U. Eberl, T. Häberle, W. Keupp, T. Langenbacher, J. Siegl, M. Volk and M.E. Michel-Beyerle, Biophys. J. Abs., 61, 837a (1992).
57. M. Friese, Diploma thesis, Technical University München (1991).
58. T.G. Ebrey and R.K. Clayton Photochem. Photobiol., 10, 109 (1969).
59. Ch. Zheng, M.E. Davis and J.A. McCammon, Chem. Phys. Lett., 173, 246 (1990).
60. A. Ogrodnik, Biochim. Biophys. Acta, 1020, 65 (1990).
61. M. Volk, T. Häberle, G. Aumeier, A. Ogrodnik, R. Feick and M.E. Michel-Beyerle, to be publ.
62. D.J. Lockhart and S.G. Boxer, Biochemistry, 26, 664 (1987).
63. A. Ogrodnik, T. Langenbacher, G. Bieser, J. Siegl, U. Eberl, M. Volk and M.E. Michel-Beyerle, Chem. Phys. Lett., in press.
64. Z.D. Popovic, G.J. Kovacs and P.S. Vincett, Chem. Phys. Lett., 116, 405 (1985).
65. C. Wraight and R. Clayton, Biochim. Biophys. Acta, 333, 246 (1973).
66. J. Breton, J.-L Martin, J.-C Lambry, S.J. Robles and D.C. Youvan, in Reaction Centers of Photosynthetic Bacteria, edited by M.E. Michel-Beyerle (Springer, Berlin, 1990), pp. 293-302.
67. N.W. Woodbury and W.W. Parson, Biochim. Biophys. Acta, 767, 345 (1984).
68. S.L. Logunov and V.Z. Pashchenko, Sov. J. Quantum Electron., 19, 88 (1989).
69. R.A. Goldstein and S.G. Boxer, Biochim. Biophys. Acta, 977, 78 (1989).
70. S.G. Boxer, D.J. Lockhart, Sh. Hammes, L. Mazzola, Ch. Kirmaier, D. Holten, D. Gaul and C. Schenck, in Current Research in Photosynthesis Vol.I, edited by M. Baltscheffsky (Kluwer, Netherlands, 1990), pp. 113-116.
71. R. Zengerle, Diploma thesis, Technical University München (1991).
72. E.J. Lous and A.J. Hoff, in The Photosynthetic Bacterial Reaction Center - Structure and Dynamics, edited by J. Breton and A. Vermeglio (Plenum Press, New York and London, 1988), pp. 71-88.
73. M. Lösche, G. Feher and M.Y. Okamura, Proc. Natl. Acad. Sci. USA, 84, 7537 (1987).
74. D.J. Lockhart and S.G. Boxer, Proc. Natl. Acad. Sci. USA, 85, 107 (1988).
75. S. Franzen, R.F. Goldstein and S.G. Boxer, J. Phys. Chem., 94, 5135 (1990).
76. M. Bixon and J. Jortner, J.Phys. Chem., 92, 7148 (1988).
77. G. Feher, T.R. Arno and M.Y. Okamura, in The Photosynthetic Bacterial Reaction Center. Structure and Dynamics, edited by J. Breton and Vermeglio (Plenum Press, New York, 1988), pp.271-287.
78. U. Eberl, Thesis, Munich (1992).
79. A. Ogrodnik, T. Langenbacher, U. Eberl, M. Volk, and M.E. Michel- Beyerle, in The Photosynthetic Bacterial Reaction Center - Structure and Dynamics II, edited by J. Breton and A. Vermeglio (Plenum Press, New York and London), in press.
80. W. Keupp, E. Baumgartner, U. Eberl, A. Ogrodnik and M.E. Michel-Beyerle, unpublished results
81. U. Eberl, M. Gilbert, W. Keupp, T. Langenbacher, J. Siegl, S.J. Robles, J. Breton, D.C. Youvan, H. Michel, A. Ogrodnik and M.E. Michel-Beyerle, in The Photosynthetic Bacterial Reaction Center - Structure and Dynamics II, edited by J. Breton and A. Vermeglio (Plenum Press, New York and London), in press.
82. W. Keupp, E. Baumgarten, U. Eberl, A. Ogrodnik and M.E. Michel-Beyerle, in preparation.